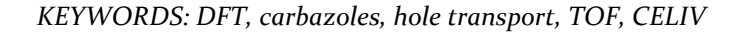
Effect of methoxy-substitutions on the hole transport properties of carbazole-based compounds: pros and cons

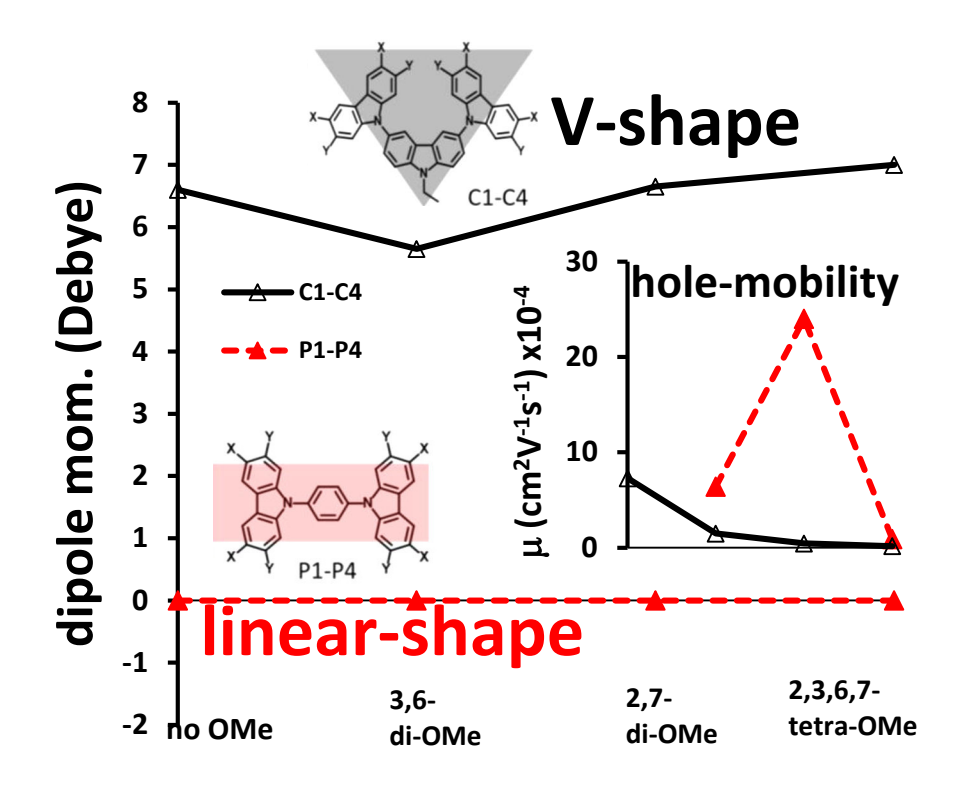
Seyhan Salman^a, Xavier Sallenave^b, Audrius Bucinkas^c, Dmytro Volyniuk^c, Oleksandr Bezvikonnyi^c, Viktorija Andruleviciene^c, Juozas Vidas Grazulevicius^{c*}, Gjergji Sini^{b*}

^aClark Atlanta University, Department of Chemistry, 223 James P. Brawley Drive, SW, Atlanta, GA, 30314.

^bCY Cergy Paris Université, Laboratoire de Physicochimie des Polymères et des Interfaces, EA 2528, 5 mail Gay-Lussac, Cergy-Pontoise Cedex, 95031, France.

^cKaunas University of Technology, Department of Polymer Chemistry and Technology, Radvilenu pl. 19, LT-50254, Kaunas, Lithuania.





Abstract

We have recently reported the role of methoxy substitutions on the optoelectronic properties of two new series of carbazole-bridge-carbazole compounds (bridge = carbazole, phenyl) by varying the number of methoxy groups from 0-4 per carbazole unit. Here, we report the effect of molecular shape (linear versus V-shape), number and linking topology of the methoxy-substitutions on the hole-transport properties of these molecules. The results indicate a delicate balance between the positive and negative effects depending on the substitution topology and the nature of the bridge. It is found that, unlike recent findings from our groups, the methoxy substituents in these compounds reduce the hole mobilities due to the enhanced molecular polarity, a detrimental effect which can be importantly reduced by designing linear D-A-D architectures. The differences in the geometries of the new compounds and their hole transport properties as a function of the nature of the bridge, number of methoxy groups and the substitution topology are explained in terms of the different symmetry of HOMO and HOMO-1 of the carbazole units, which interact very differently with the methoxy substituents and the bridge (carbazole or phenyl). The pros and cons of using-versus-avoiding methoxy groups in order to improve the hole mobility of the new compounds are discussed with regard to the targeted application.

1. Introduction

In the domain of organic electronics, the design of new organic semiconductors progresses through the introduction of new architectural concepts, based on known and/or new building groups. The properties of the building groups can subsequently be fine-tuned through linking of different small groups instead of hydrogens atoms. Among numerous well-known building blocks, we focus here on the carbazole due to its excellent hole-transport properties, as well as its remarkable thermal, optical, photochemical, and chemical stability. Such accumulation of interesting properties makes carbazole-based materials one of the preferred choices as active material in a variety of organic electronic devices such as organic light-emitting diodes (OLEDs)¹⁻⁴ and solar cells.⁵⁻⁸ Moreover, carbazole-based materials can be easily functionalized by several substituents to modulate their optical and electronic properties.⁹⁻¹⁰ For instance, carbazoles commonly

functionalized through C3,C6-, C2,C7-, and N-9 positions have been reported for application in organic light-emitting diodes¹¹⁻¹³ and photovoltaic devices.¹⁴⁻¹⁷ However, each introduced substituent is expected to induce more than only one effect, thus tuning simultaneously, sometimes in an undesirable way, several properties of carbazole such as its redox, optical, charge-transport, and photovoltaic properties. The overall result then depends on the weight of each effect, which in turn depends on the nature of the molecular core, linking topology, and the number of substituents. In the following discussion, we focus on the effect of the methoxy group on the hole-transport properties of carbazole-based compounds, given their extensive use in tuning the material properties used in organic electronics.

Several studies have reported the effect of the methoxy groups on the hole-transport properties of amorphous compounds in general¹⁸⁻²⁴ and in carbazole-based ones.²⁵⁻²⁶ However, while the substitution pattern has shown to significantly affect these properties, no systematic analysis of these substitutions on the hole-transport properties of these compounds has been done. The number of methoxy groups per carbazole unit, also allowing fine-tuning the target properties, has not yet been addressed in a systematic way.²⁷ The presence of four methoxy groups per carbazole unit, for instance in positions C2, C3, C6, C7 is expected to prevent their free orientation, hence reduce the disorder stemming from this effect, but at the same time is expected to significantly affect the local electrostatic polarizations, thus increase the density of states (DOS) for the charge transport and reduce their mobility.

From a general standpoint, it is important to highlight that increasing of charge mobility of semiconductors constitutes the main targeted property in order to increase the device performances. This is particularly true but quite delicate in the case of perovskite solar cells (PSC), where huge research efforts are focused on replacing spiro-OMeTAD by new hole transporting materials (HTM) exhibiting larger hole mobility. Indeed, recently Sallenave *et al.*²⁸ showed that just replacing methoxy groups of spiro-OMeTAD by methyl groups (spiro-MeTAD) resulted in a significant increase in hole mobility by more than five times, but maintains the photovoltaic performances of PSC slightly lower as compared to spiro-MeTAD-based PSCs, thus pointing to the dominant importance of perovskite-HTM

interface properties and to the special role of methoxy groups in this regard. Replacing the methoxy groups in order to increase the hole mobility of semiconductors should consequently be considered with care when it comes to use the new materials as HTMs in PSCs. A good strategy could then be to keep the methoxy groups in the molecules but play with the molecular-design architecture in order to avoid the detrimental effect of the polarity associated to the methoxy groups.

In an aim to obtain deeper insight on these aspects, we have recently reported on six new donor-acceptor-donor (D-A-D) type compounds containing methoxy-substituted carbazoles as donor fragments, linked to phenyl and carbazole bridges (acceptors) in a linear (para-phenyl) or V-shape (3,6 positions of carbazole) architectures.²⁹ The lateral carbazole fragments of both compounds contain 0-4 methoxy groups linked at the C2, C3, C6, C7 positions. The new compounds (reported hereafter as C1-C4 and P1-P4 for the triscarbazole- and phenyl-biscarbazole-based series respectively, see Scheme 1) showed interesting differences in the redox and photophysical properties, mainly due to the absence and presence of molecular dipole moments in the case of linear- and V-shape D-A-D molecular architectures, respectively. Upon methoxy substitutions, interesting dependence of photophysical properties on the number and linking position of the substituents were also observed.²⁹

Here, we report the effect of the number and linking topology of methoxy groups on the charge mobility of compounds C1-C4 and P1-P4, given their potential use in OLED or PSC applications. To this aim, we apply a series of experimental and density functional theory (DFT) methods to address the structure-property relationship of these compounds. The results indicate strong dependence of the hole mobility on both the linear versus V-shape D-A-D architecture, as well as the number and linking topology of the methoxy substitutions. In agreement with previous reports, ¹⁹ the methoxy groups are found to have an important role on the hole mobility by means of a subtle interplay between two counteracting effects: the positive effect (mobility increase) due to an increase in the strength of intermolecular interactions, and the negative effect (mobility decrease) due to an increase in the molecular (and bulk) polarity.

Scheme 1. Molecular structures of the carbazole trimers with N-ethylcarbazole C1-C4 or phenyl P1-P4 core.

2. Experimental section

2.1 Synthesis

The compounds C1-C4 are synthesized as previously described²⁹ from the reaction of carbazole derivatives, CuI, and 18-crown-6 in a solution of N-ethyl-3,6-dibromocarbazole in dry DMF. Similarly, Compounds P1-P4 are synthesized by adding carbazole derivatives, CuI, K₃PO₄, and trans-1,2diaminocyclohexane in a solution of 1,4-diiodobenzene in dioxane.

2.2 Hole mobility measurements

Time of flight method $(TOF)^{30}$ and carrier extraction in linearly increasing voltage $(CELIV)^{31}$ methods were exploited for the charge carrier mobility (μ) measurements of vacuum deposited layers. Both TOF and CELIV experimental setups consisted of a pulsed

Nd:YAG laser (EKSPLA NL300), a Keithley 6517B electrometer, a Tektronix TDS 3052C oscilloscope and functional generator AFG3011C. To detect the onset of the laser pulse by a DET10A/M Si based detector for synchronization with a digital storage oscilloscope Tektronix TDS 3032C, the light pulse was split into two beams. TOF photocurrent transients at the different surface potentials (for detecting both holes and electrons) at the moment of photogeneration were recorded by an oscilloscope. The transit time (tt) with the applied bias (V) indicated the passage of charges through the entire thickness (d) of the samples. TOF hole mobility was calculated as μ =d²/U·tt. CELIV hole mobility was calculated as: μ =2d²/At_{max}², where A=U(t)/t is the voltage rise rate; t_{max} is the time for the current to reach its extraction maximum peak (seen as the maximum on photo-CELIV transient pulses in Figures 3b and S2); and d is the sample thickness.

2.3 Computational methodology

The optimized geometries and relevant energies of the carbazole derivatives were obtained by means of density functional theory (DFT)³² calculations with the implicit consideration of the dielectric (ϵ) environment via the conductor-like polarizable continuum model³³⁻³⁶ (CPCM)/DFT in diethylether by using the range-separated ω B97XD³⁷ functional and the 6-31G** basis set. An iteration procedure described by Sun *et al.*,³⁸ was employed to tune the range-separation parameter ω , by incorporating the solvent effect (diethylether, ϵ =4.12). Similar ω values around 0.012 bohr⁻¹ was found for all compounds, which are much smaller than the default value (0.2 bohr⁻¹). The tuned- ω *B97XD functional with a constant value (ω *=0.012bohr⁻¹) was used in this study for all compounds. Test calculations with the default ω B97XD and B3LYP³⁹⁻⁴⁰ functionals were also performed for comparison reasons. The intramolecular reorganization energies (λ) of the compounds were directly calculated from the adiabatic potential-energy surfaces (PESs) of the neutral and charged species, following the usual practice.⁴¹ All calculations were performed with the Gaussian09 software (Revision B1).⁴²

3. Results and Discussion

3.1 Structural and electronic properties

Inter-ring dihedral angles. The optimized ground state geometries of the compounds C1-C4 and P1-P4 are shown in Figure 1a. The arrows drawn in compounds C2, C3, P2, P3 indicate the orientation of the methoxy groups corresponding to the lowest energy conformer. The conformers corresponding to methoxy orientations along the opposite directions with respect to those shown in Figure 1a are higher in energy by 2.4 kcal/mol in the case of C2 and P2, and 2 kcal/mol in the case of C3 and P3.

The dihedral angles between the lateral carbazole units and the central core are in the range of 86.5-89.4° and 70.0-89.1° for compounds C1-C4 and P1-P4 respectively. A detailed analysis of the factors that determine these geometrical properties is provided in the Annex I and Figure S1 in the Supporting Information (SI). The main conclusions from this analysis highlight two aspects: (i) the large dihedral angles close to orthogonality are not dominated by steric interactions but by inter-fragment interactions. (ii) The inter-fragment interactions are dominated by the destabilizing 4-electron interactions as compared to stabilizing 2-electron ones. In the case of C-series of compounds, the 4-electron interactions are weaker at the orthogonal geometry, which explains the practically orthogonal inter-fragment orientation in these compounds. In the case of P1-P4, the 4-electron interactions are stronger at the orthogonal geometry, which explains the smaller dihedral angles for these compounds. The rotational potential around the inter-ring bonds are almost flat between 70°-90°, see Figure 1b. These results suggest an important role of geometrical disorder on the hole-transport of these compounds.

Molecular orbitals. A selected set of calculated molecular orbitals for compounds C1-C4 and P1-P4 corresponding to the highest occupied molecular orbitals (HOMO) and the lowest unoccupied molecular orbitals (LUMO) are shown in Figure 1c. The calculated HOMO and LUMO energies of all compounds are tabulated in Table S1, Supporting information (SI). All HOMOs are localized on the lateral carbazole fragments; whereas, LUMOs are mainly localized on the central fragment (except for P1 and P2). One important result here is that, the HOMO (HOMO-1) wave function distribution depends on the positions of the methoxy-substitution on the carbazole moiety. The HOMO (HOMO-1) wave function symmetry with respect to the plane of the central fragment indicates symmetric orbitals for the non-substituted and 3,6-substituted compounds (C1, C2, P1, P2);

whereas, antisymmetric orbitals for the 2,7-and tetra-OMe substituted compounds (C3, C4, P3, P4). A detailed discussion on this aspect of orbital symmetry can be found elsewhere.²⁹

The important observation of HOMO wave function symmetry is the missing of the through-bridge π -conjugation for most compounds. This could be related to the quasi-orthogonal inter-ring geometry configurations resulting from our calculations. However, while this factor can explain the absence of through-bridge π -conjugation in C1-C4 compounds, comparison between HOMOs of P1 and P4, both compounds exhibiting identical dihedral angles of 84°, points to the impact of a symmetry mismatch between the local HOMOs of the lateral carbazoles and the bridge.

From the energy point of view, degenerate HOMO and HOMO-1 were found for almost all compounds, again due to the missing through-bridge π -conjugation. Both the degeneracy and the different symmetries of the HOMO and HOMO-1 across and between the two series of compounds will have an important effect on the transport properties of these compounds, as will be discussed in the following sections.

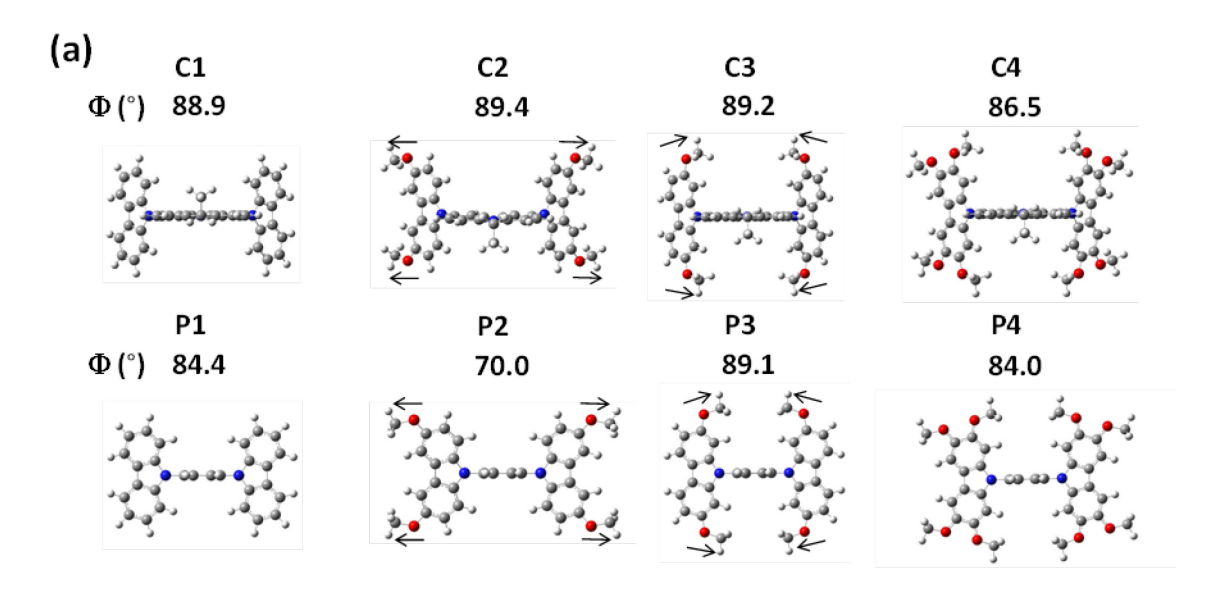
It is worth remembering here that the contribution of both lateral carbazoles, for instance, in the HOMOs of C1-C4, is an artefact of the tendency of all DFT methods towards over-delocalization of the molecular orbitals. In these cases, the degenerate HOMO and HOMO-1 should be strictly localized only on the left and right carbazole moieties, respectively. On the contrary, in the case of HOMO of P1 and P2, due to the collective effect of twisted geometry (dihedral angle of 70° in P2) and local carbazole HOMO symmetry (symmetric with respect to the phenyl plane), some orbital contribution from the bridge is obvious in Figure 1c, making HOMO and HOMO-1 delocalized throughout the entire molecule. As we will show later, this difference in HOMO distributions will be very important for the discussion of the trends in the hole mobility of these compounds.

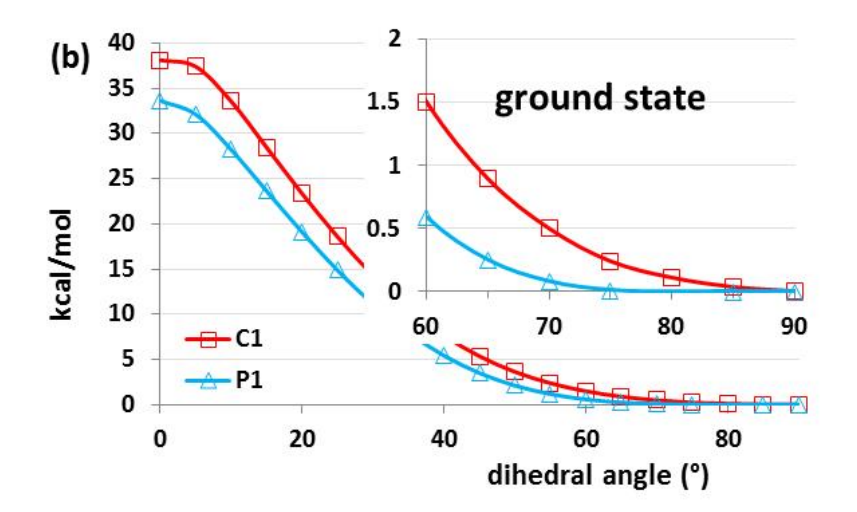
As expected, the increase of HOMO energies through C and P series of compounds can be seen in Figure 1d, which stems from the (antibonding) conjugation between the oxygen lone pair of the methoxy groups with the π -system of carbazole moieties. This effect is larger for the 3,6-substituted compounds than the 2,7-substituted ones, due to the presence and absence of HOMO coefficients at 3,6 and 2,7 positions in carbazole, respectively (see

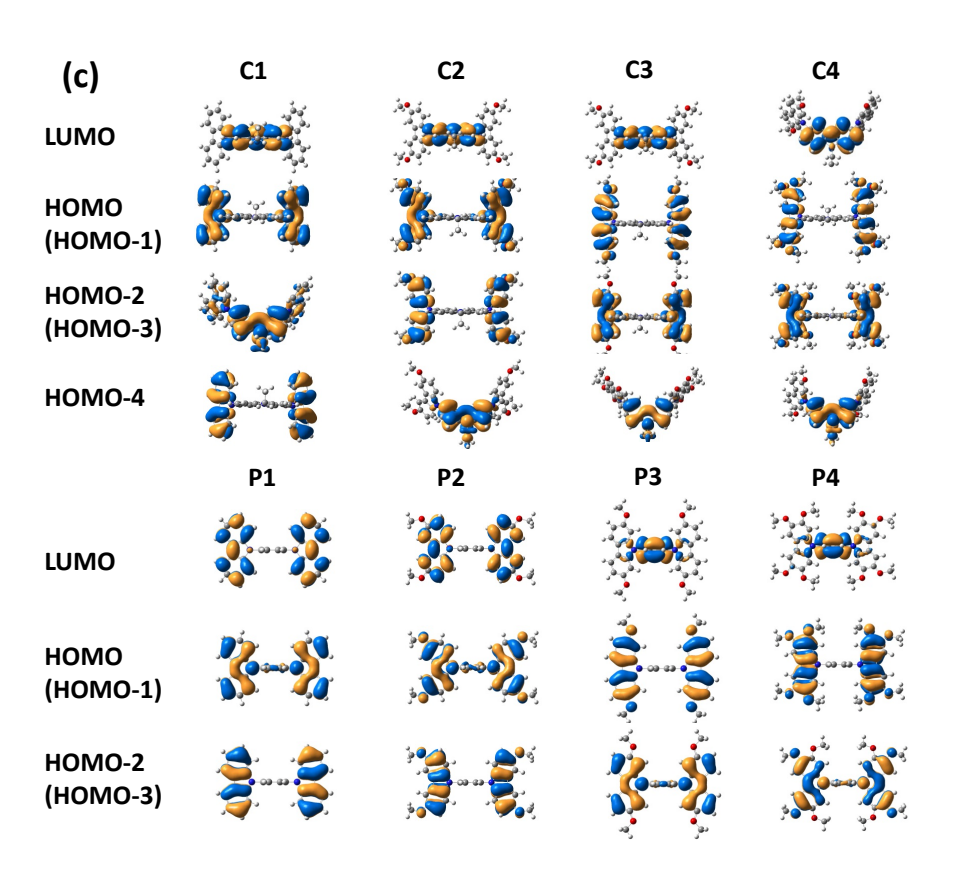
Figure S1a). The cumulated effect of four methoxy groups in C4 and P4 is thus dominated by the 3,6 substitutions.

Finally, we report here one result from our previous study on these compounds²⁹ compared to the non-substituted compounds C1 and P1, 3,6-OMe substitutions reduce the HOMO-LUMO gap (redshift the lowest optical absorption band), whereas 2,7-OMe substitutions increase it. In the case of tetra-OMe substituted compounds C4 and P4, some cancellation of the two opposite effects occurs, the total result being only slightly dominated by the impact from 2,7-OMe group.

Dipole moments. An important difference between the C and P compounds stems from their different dipole moments. Owing to the V-shape of the triscarbazole, the dipole moment of compound C1 is larger than the free carbazole (6.6 and 2.5 Debye for triscarbazole and carbazole, respectively). Compared to the unsubstituted compound C1, the presence and orientational freedom of methoxy groups in C2 and C3 results in a large disorder in dipole moments, peaking at roughly 11 Debye in the case of compound C3. On the contrary, the linear D-A-D linking in P1-P4 compounds results in zero net dipole moment for all these compounds due to the total cancelation of the local carbazole dipole moments. Consequently, the impact of the substitution topology on the hole transport properties of these compounds is expected to be different for C1-C4 and P1-P4 series.







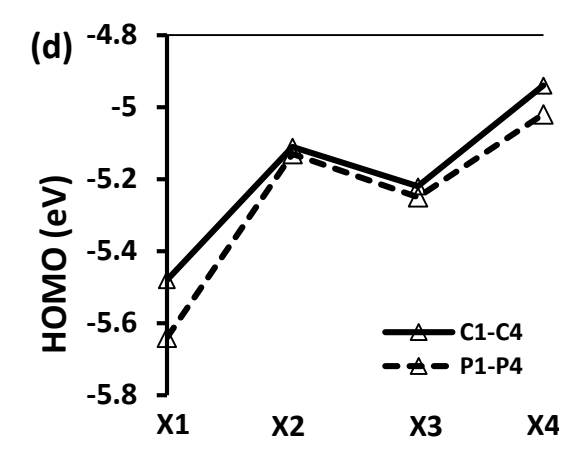


Figure 1. (a) Optimized ground state geometries of compounds C1-C4 and P1-P4. The numbers correspond to the dihedral angles (Φ, in degree) between the lateral and central groups. (b) Evolution of the ground state energy of compounds C1 and P1 as a function of the inter-ring dihedral angles. The results are obtained by means of scan calculations with full geometry optimization at each point. The energy corresponding to dihedral angle of 90° is taken as energy reference for each molecule. (c) Representations of HOMO-4 through LUMO orbitals corresponding to compounds C1-C4 and P1-P4. All results were obtained at CPCM-tuned ωB97XD/6-31G(d,p) level by considering diethylether (ε =4.24) as a polarizable medium (solvent effect). (d) Evolution of the HOMO energy of compounds C1-C4 and P1-P4 (where X = C, P).

3.2 Charge transport properties

Time of flight (TOF)³⁰ and carrier extraction in linearly increasing voltage (CELIV)³¹ measurements were used to estimate the charge-transport properties of vacuum deposited films of compounds C1-C4 and P1-P4. The corresponding electric field dependencies are shown in Figure 2, indicating hole-mobility values ranging between ca. 8.5×10⁻⁷-2.8×10⁻³ cm²/Vs (at electric fields of 0.5×10⁵ - 5.5×10⁵ V/cm). The hole transit times for the C and P compounds were well seen on log-log plots of TOF transients which displayed even low dispersity of hole transport for compounds C2 and P2 (Figure 3a and Figures S2 & S3). On photo-CELIV transient pulses, the maximum required mobility values by CELIV were also well seen (Figure 3b and Figure S2). TOF measurements at different electric fields and temperatures were also conducted, allowing to deduce several parameters in the framework of Gaussian disorder model (GDM),⁴³ according to the following equation:

$$\mu = \mu_0 \exp[-(\frac{2\hat{\sigma}}{3})^2] \exp[C(\hat{\sigma}^2 - \Sigma^2)E^{\frac{1}{2}}]$$
(1)

Here, $\hat{\sigma} = \sigma/kT$, σ is the energy width of the hopping site manifold, Σ is the positional disorder, and C is a constant. Additional details can be found in Annex II, SI.

The results are plotted in Figures S4-S6, whereas a set of hole mobility parameters deduced from these measurements as previously described by Mimaite *et al.*¹⁹ are summarized in Table 1.

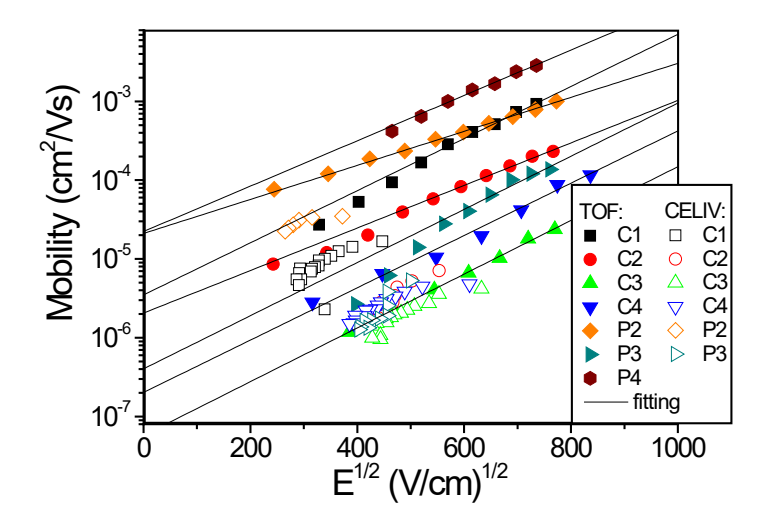


Figure 2. Electric field dependence of the hole and electron drift mobility for the layers of compounds C1-C4 and P1-P4 at room temperature. The samples for the measurements were prepared by the vacuum deposition technique.

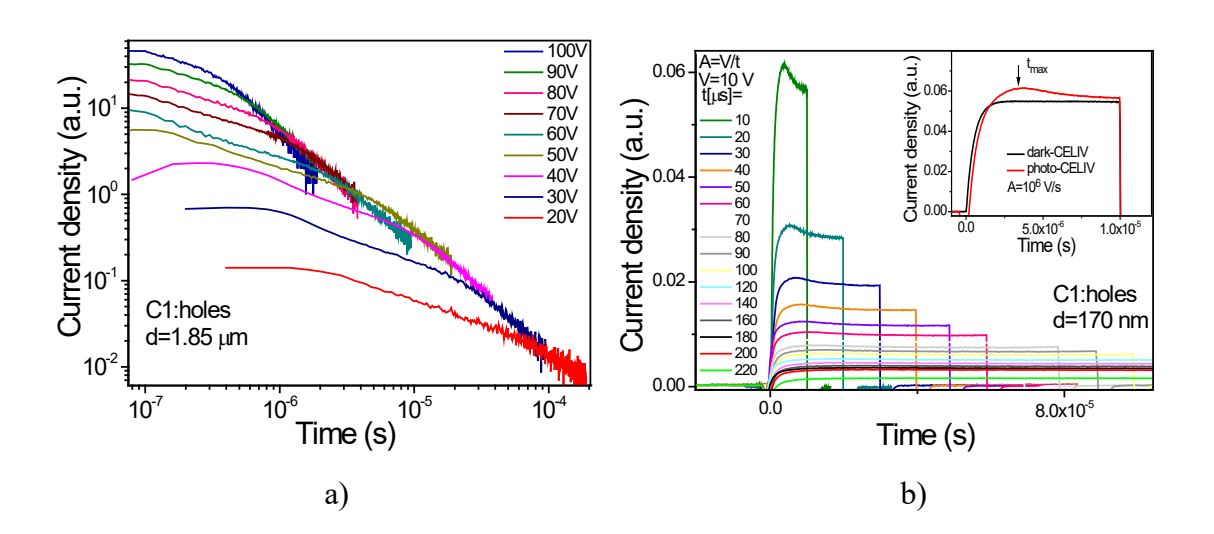


Figure 3. TOF (a) and Photo-CELIV (b) current transient pulses of holes for the layer of C1 at different electric fields at room temperature. Insert: Darck-CELIV and photo-CELIV current transient pulses at the voltage rise rate (A) of 10⁶ V/s.

Table 1. Time of flight (TOF) hole mobility parameters^a (μ , μ ₀, σ , Σ) of the vacuum deposited layers of compounds C1-C4 and P1-P4 along with the HOMO energies (E_{HOMO}), dipole moments (DM) in the ground state of the neutral species, isotropic polarizabilities (α), and intramolecular reorganization energies (λ) for hole transport obtained at the CPCM-tuned ω B97XD/6-31G**in diethylether.

| Cmnd | $E_{\rm HOMO}$ | λ | DM | α | μ (10 ⁻⁴) | μ0 | σ | Σ |
|-------|----------------|-----|--|-------------------|-----------------------|--------------------|-----|-----|
| Cmpd. | eV | meV | Debye | Bohr ³ | $cm^2V^{-1}s^{-1}$ | $cm^2V^{-1}s^{-1}$ | meV | |
| C1 | -5.57 | 385 | $6.6^{\rm b}$ / $2.2^{\rm c}$ / $3.8^{\rm d}$ | 585 | 7.3 | 0.138 | 125 | 3.6 |
| C2 | -5.11 | 233 | $2.7^{\rm b} (8.6)^{\rm b} / < 2^{\rm c}$ | 585 | 1.5 | 0.861 | 138 | 3.6 |
| С3 | -5.21 | 194 | 11 ^b (2.3) ^b / 11.2 ^c / 19.6 ^d | 592 | 0.45 | 0.056 | 136 | 3.3 |
| C4 | -4.94 | 194 | $7.0^{\rm b}$ / $1.7^{\rm c}$ / $2.9^{\rm d}$ | 618 | 0.17 | 0.023 | 138 | 3.3 |
| P1 | -5.66 | 260 | 0.0^{b} | 418 | - | - | - | - |
| P2 | -5.16 | 196 | 0.0^{b} | 454 | 6.4 | 0.051 | 107 | 2.9 |
| P3 | -5.29 | 192 | 0.0^{b} | 448 | 24 | 0.016 | 98 | 1.6 |
| P4 | -5.02 | 195 | 0.0^{b} | 482 | 0.9 | 0.022 | 126 | 3.9 |

^aHole and electron mobility values measured at electric field of 6.4×10⁵ V/cm.

^bTheoretical estimations for the dipole moments of compounds C1-C4. The two sets of dipole moments for compounds C2 and C3 correspond to two opposite orientations of methoxy groups in each carbazole unit; the values in parentheses correspond to the less stable conformer (by roughly 2.4 and 2.0 kcal/mol for C2 and C3, respectively).

^cExperimental values of dipole moments for compounds C1 – C4 as determined by using Bakshiev polarity function. ⁴⁴ See Annex III (SI) for details.

^dExperimental values of dipole moments for compounds C1, C3, C4 as determined by using Lippert-Mataga plot.⁴⁵⁻⁴⁷ See Annex III (SI) for details.

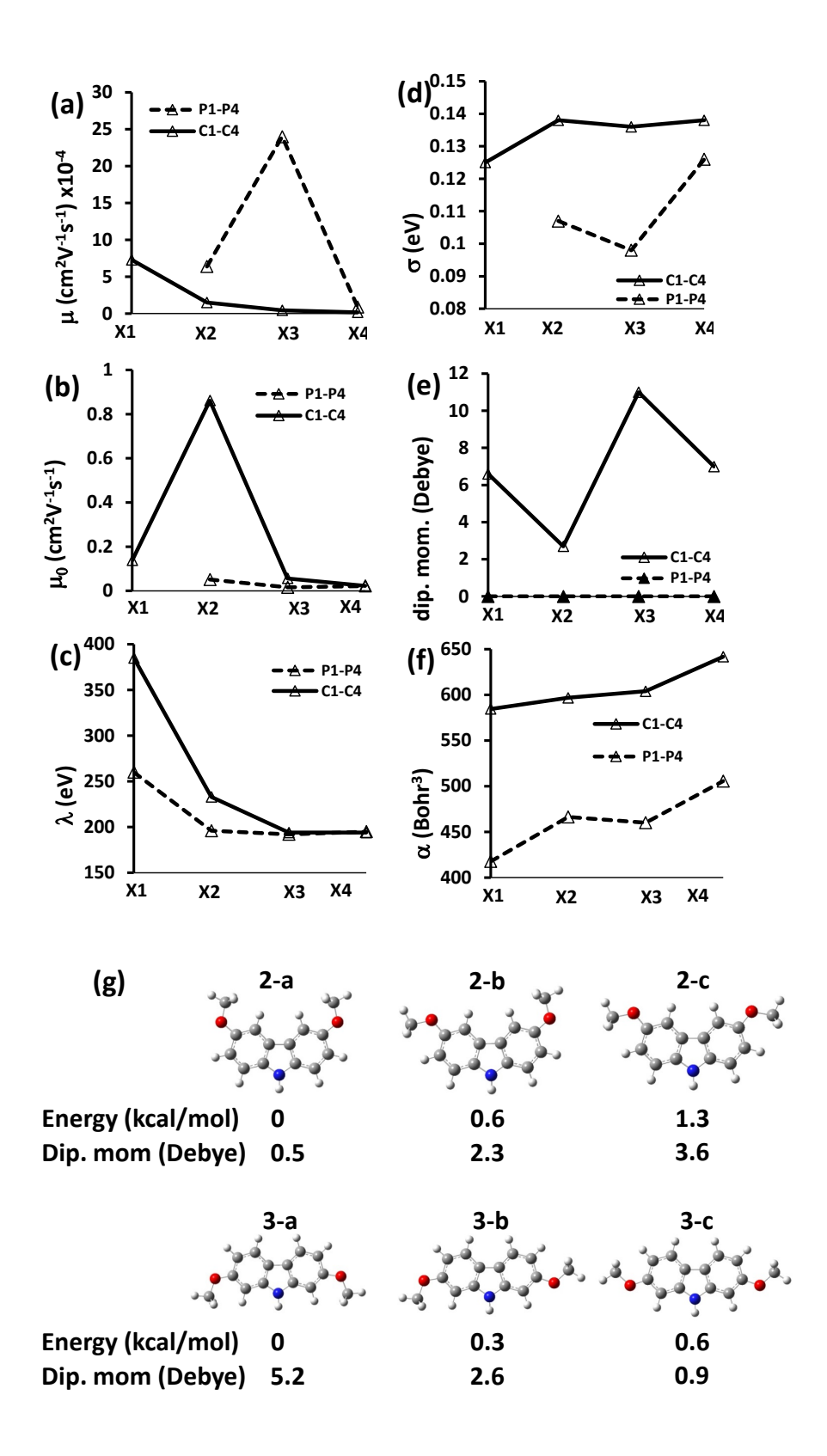


Figure 4. Evolution of the (a) hole mobility, μ , (b) zero-field hole mobility, μ_0 , (c) intramolecular reorganization energy, λ , as obtained from DFT calculations at the CPCM-tuned ω B97XD/6-

 $31G^{**}$ "in diethylether" level, (d) energy disorder parameter, σ , (e) dipole moments, (f) isotropic molecular polarizabilities, α , across the series of compounds C1-C4 and P1-P4 (where X=C, P) and (g) relative total energies and dipole moments corresponding to different methoxy orientations in the dimethoxy-substituted free carbazole. The parameters μ , μ_0 , and σ were deduced from TOF measurements at different electric fields and temperatures. The lines have no physical meaning and are only guides for the eye.

As a preliminary conclusion on these results, we highlight the better charge transport of P compounds as compared to C ones, and the decrease in the hole mobility of the methoxy-substituted compounds C2-C4 as compared to the non-substituted C1 compound (Figure 4a). The missing hole mobility for compound P1 prevents us to make a similar comparison in the P series of compounds.

3.2.1 Polarity versus intermolecular interactions

In order to understand the trends of the hole mobility in these compounds, we discuss firstly the competition between two effects, the polarity of the compounds and the strength of the intermolecular interactions between adjacent molecules.

Firstly, we focus on the polarity factor. It is well established that, as dipole moment disorder and in general the polarization power increases, the energy disorder parameter σ increases and the charge mobility decreases. ^{21-24, 48-49} (See Annex IV for a quick sketch on the logical correlation between dipole moments and the charge mobility). The theoretical and experimental estimates of dipole moments are shown in Table 1, indicating similar trends in the order C3 > C4 > C1 > C2. Since all triscarbazole-based compounds C1-C4 exhibit considerable dipole moments, ranging from 2.2 to more than 11.2 Debye (Table 1), the polarity factor is expected to significantly affect the hole mobility of compounds C1-C4.

The presence of dipole moments in C1-C4 compounds is due to three contributions: (i) the presence of small dipole moments in each carbazole core (ca. 2.1 Debye); (ii) the impact of the polar methoxy groups; and (iii) the V-shape of compounds C1-C4 (Scheme 1), which enhances the dipole moment of the triscarbazoles by adding the contributions stemming from each fragment.²⁹ Compared to C1-C4, compounds P1-P4 exhibit zero net dipole

moments as a result of the linear D-A-D molecular architecture; thus, it is anticipated that their hole mobilities should remain almost unaffected from polarity changes. Based on the differences in dipole moments, better hole transporting properties should be expected for compounds P1-P4 as compared to C1-C4, which seems consistent with the experimental results.

With regards to the interaction energy (IE) factor, it has been recently reported that strong intermolecular interactions can help reducing the intramolecular geometrical disorder, thus reducing the HOMO energy distribution (disorder) and increasing the hole mobility. ¹⁹ Note that the IE factor becomes important only when HOMO is delocalized over different molecular fragments, in which case geometrical deformations could play a role for the HOMO energy disorder.

The methoxy groups have the potential to induce both effects, i.e., increase the dipole moments and increase the intermolecular interaction energy. The global result should then depend on the weight of each factor in a given molecule. The decrease of the hole mobilities in the case of methoxy-substituted C2-C4 compounds as compared to the nonsubstituted compound C1 indicates that, in terms of the two factors mentioned above, the effect of increased dipole and polarization disorder induced by methoxy groups is dominating over the effect of increased intermolecular interaction strength. As shown above, this stems from the strong HOMO localizations on the carbazole moieties alone (see Figure 1c), making HOMO energy almost insensitive to the changes in dihedral angles, hence insensitive to the impact of the interaction strength on the geometrical and energy disorder. In the case of P compounds, we are unable to make a similar discussion due to the lack of the hole mobility value for the unsubstituted compound P1.

3.2.2 Disorder versus polaronic hole transport

We now turn our attention to the impact of the polaronic transport on the hole mobility of these compounds. In the framework of GDM model (equation 1), the potential contribution of the polaronic hole transport to the hole mobilities can be deduced from the zero-field hole mobility parameter, μ_0 (Table 1 and Figure 4b). This parameter basically depends on

the molecular parameters such as reorganization energy and transfer integrals between the adjacent molecules. As collected in Table 1, large μ₀ values in the range of ~0.02-1 cm² V⁻ ¹s⁻¹, suggests molecular parameters suitable for hole transporting materials. Interestingly, the μ_0 value of compound C1 (0.138 cm² V⁻¹ s⁻¹) is larger than those of compounds C3, C4, P2-P4 (in the range of 0.016-0.056 cm² V⁻¹ s⁻¹), despite its much larger intramolecular reorganization energy (385 meV for C1 and 192-260 meV for P-compounds). This dichotomy is consequently intriguing, suspected to stem from the differences in the electronic couplings between HOMOs in adjacent molecules. Indeed, in the solid films of these compounds, large deviations from the quasi-orthogonality of the interring dihedrals could be predicted, given that interring torsion barriers smaller than 1 kcal/mol were found for all compounds between 65-90° (Figure 1b). Because of the orbital-symmetry differences discussed above, a space extension over the whole molecular backbone can be expected in the case of HOMO of C1 (symmetric with respect to the central carbazole plane), but not in the case of C3-C4 and P3-P4 (antisymmetric). Accordingly, in the case of C1, we would expect larger potential for efficient HOMO-HOMO overlaps and electronic couplings, which could explain the large μ_0 value of C1.

Despite the favorable molecular characteristics suggested for all compounds by the μ_0 values as tabulated in Table 1, much smaller hole mobilities (μ) (i.e., by 10^{-2} - 10^{-3} times smaller) as compared to μ_0 were deduced from TOF measurement, indicating hole transport is being dominated by other factors as compared to the previously discussed ones. Indeed, the comparison between Figure 4a (μ) and Figure 4b (μ_0) clearly indicates strong discrepancies between the evolutions of the two parameters (μ and μ_0) across the series of compounds. The evolution of the theoretical intramolecular reorganization energies (λ , Figure 4c) supports the experimental results only for the C series but fails to explain the trend of μ in the case of P compounds (Figure 4a) and the trend μ_0 (Figure 4b) in the case of C compounds. Similarly, efforts to estimate somehow the strongest transfer integrals in the case of compound P2 in crystalline state result in small values (ca. 7 and 17 meV, see Annex V, SI), supporting the idea that the transfer-integral variations in the amorphous films of C1-C4 and P1-P4 should be unable to explain the corresponding trends of the hole mobilities. It can be safely concluded from the above comparisons that the contribution of

the intramolecular reorganization energies and of the transfer integrals between adjacent molecules (polaronic transport) to the hole mobility trends in the solid films of compounds C1-C4 and P1-P4 is negligible, which, as shown below, is directly pointing to the dominance of other phenomena in the hole mobility values.

Energy disorder parameter (σ). We now turn our discussion to the effect of methoxy groups on the energy disorder parameter (σ). As can be seen from Table 1, energy disorder parameter increases by ca. 10-13 meV for methoxy-substituted C2-C4 compounds as compared to the unsubstituted C1 compound, indicating negative global effect of the OMe groups. Intriguingly, the σ values remain almost constant for C2-C4 (Figure 4d), despite the strong variations in their dipole moments (Figure 4e). Both findings indicate that: (i) the geometrical deformations affect very weakly the HOMO energy disorder due to the strong HOMO localization in the rigid planar carbazole unities (compounds C3 and C4). This is also supported by the identical HOMO and HOMO-1 energies in both compounds; (ii) the variation in the polarity and polarizability should be negligible, meaning that the global impact of the dipole moments exhibits negligible variation between the di- and tetra-OMe-substituted carbazole.

In order to understand this trend, we focus on the comparison between C1 and C2 compounds. Results in Table 1 indicate an increase in σ from 125 to 138 meV for C1 and C2, respectively (Table 1), despite the decrease in dipole moments from 6.6 D to 2.7 D in the same order (Table 1 and Figure 4e). Additionally, the strength of the intermolecular interaction is expected to increase from C1 to C2 due to the presence of methoxy groups, which was shown to improve the hole mobility. Finally, to make this mystery darker, the zero-field hole-mobility parameter, μ_0 , is found to be larger for C2 than for C1 (Figure 4b), in agreement with the much smaller intramolecular reorganization energy for C2 (Table 1 and Figure 4c). We note that the medium reorganization energy is also expected to be smaller for C2 given the smaller dipole moment of this compound as compared to C1.

All these "standard" parameters suggest consequently larger hole mobility for C2 as compared to C1, which is at odds with the experimental result. A possible explanation to

this dichotomy could be the presence of different conformers for compound C2, corresponding to different orientations of the methoxy groups (Figure 1a). Indeed, one possible "limit" conformer for compound C2 (presenting methoxy orientation along the opposite directions with respect to those shown in Figure 1a) is higher in energy by 2.4 kcal/mol as compared to the more stable one, and exhibits a dipole moment of 8.6 Debye. Additionally, conformers presenting irregular methoxy orientations in between the two limit cases should be closer in energy, hence in thermal equilibrium with the lowest-energy one. Some examples in the case of dimethoxy-substituted free carbazole are shown in Figure 4g, top panel. We speculate consequently that a distribution of dipole moments ranging \sim 2-9 Debye could be supposed to exist in the films of compound C2, obviously resulting in larger σ value and smaller hole mobility for this compound as compared to C1.

In the case of compound C3, energy differences between conformers differing by methoxy space orientations are even smaller (Figure 4g, bottom panel), indicating that large disorder in the methoxy space-orientations for compound C3 could be easily achieved by means of thermal agitation, again suggesting large distribution on the dipole moments. As for compound C4, the orientation of the methoxy groups is constricted by the steric hindrance between them. The larger σ of C4 than that of C1 could then be due to the largest isotropic polarizability found for compound C4 (Figure 4f).

Based on these observations in the C series, we conclude that the effect of the methoxy groups in the σ parameter of these compounds dominated through two main effects: (i) increase in dipole moments, thus increasing the energy disorder, and (ii) HOMO localization on rigid planar moieties of C compounds, making the HOMO energy insensitive to the geometrical deformations, thus reducing the energy disorder.

In terms of the P compounds, large deviations in σ values are obtained across the series, meaning that the change of the bridge from carbazole to phenyl induces important results: (i) The one-by-one comparison indicates smaller sigma values for the P series. Globally, this should be due to the absence (zero) of total dipole moments. (ii) Across compounds

P2-P4 the three σ values vary importantly, as opposed to identical values found for C2-C4. The smaller σ value (and the larger hole mobility) corresponds to P3, in which degenerate HOMO and HOMO-1 are strictly localized on only one carbazole moiety. Compared to P3, very efficient bridging between the two carbazole moieties can be obtained in HOMO of P2 (Figure 2), which is supported by the important energy splitting (0.24 eV) between HOMO and HOMO-1. In the case of P4, HOMO and HOMO-1 are degenerate, but HOMO-2 is situated only 0.02 eV lower in energy (less than kT), thus being directly involved in the hole transport. Both P2 and P4 are consequently sensitive to the geometrical deformations, explaining their larger σ values as compared to P3.

4. Discussion and Conclusions

Our results suggest that (i) the charge transport in P compounds is enhanced as compared to C ones; (ii) the hole mobility of the methoxy substituted compounds C2-C4 decreases as compared to the non-substituted one C1; and (iii) the energy disorder factor dominates the absolute values and trends in hole mobility through the series.

Previous studies^{19, 28} have established that the impact of methoxy groups on the hole mobility of organic semiconductors results from a tradeoff between two main factors: (i) the detrimental impact of the increased molecular polarity (permanent dipole moments) and bulk polarization effect; and (ii) the positive effect of the increased interaction strength between adjacent molecules. Strong interactions between molecules were found to favor an increase in the hole mobility by means of reducing the geometrical disorder and HOMO energy distribution, hence through the reduction of the corresponding contribution to the energy disorder. Interestingly, the impact of methoxy substitutions on the hole mobility of compounds C1-C4 and P1-P4 was found to be detrimental. Our analysis shows that, while the methoxy groups do enhance the detrimental polarity factor in compounds C2-C4 as compared to the non-substituted C1, the positive impact of the IE factor is switched off because of the HOMO localization in only one rigid carbazole fragment. Switching "on" the IE factor in order to overcome the detrimental polarity effect of methoxy groups consequently suggests the design of semiconductor architectures that have HOMO

distribution among different molecular fragments.

Comparison between series C1-C4 and P1-P4 also shows that the detrimental impact of the polarity factor on the hole mobility can be reduced by designing linear- versus V-shape D-A-D semiconductors: P2-P4 compounds with carbazole groups linked in para-position of a phenyl bridge exhibit larger hole mobilities as compared to their C2-C3 counterparts (3,6-linked triscarbazoles) due to the zero dipole moments in centro-symmetric P1-P4 compounds.

The impact of the substitution topology is not straightforward and depends on the nature of the bridge between the two lateral carbazole moieties. The local carbazole HOMO in 2,7-substitutions is antisymmetric with respect to the plane of the bridge, as opposed to symmetric local HOMOs in the case of 3,6-substitutions (Figure 1c). This difference in carbazole's local HOMO symmetry affects two important parameters: the inter-fragment orbital symmetry mismatch, and the inter-fragment dihedral angles, the second parameter being also dependent on the first one. In the case of 2,7-substitutions, quasi-orthogonal inter-fragment geometry is preferred independently of the nature of the bridge. In the case of 3,6-substitutions, the interring dihedrals depend on the nature of the bridge: still orthogonal geometry is preferred in the case of compounds C2 (carbazole bridge), as compared to the twisted geometry in the case of P2 (phenyl bridge). These differences are maintained in the case of tetra-OMe substituted compounds C4 and P4. As a result of structural and orbital symmetry factors, the impact of the substitution topology and the number of substituents on the hole mobility is practically absent in the case of carbazole bridge (compounds C2-C4); whereas, significant effect is observed in the case of phenyl bridge. In the latter case, HOMO (HOMO-2) extension over the entire molecule becomes possible in the presence of methoxy groups in the 3,6-positions in P2 (P4), causing the HOMO (HOMO-2) energy being sensitive to the geometrical deformations, in turn increasing the energy disorder and decreasing the hole mobility. This effect (throughbridge pi-conjugation) is absent in the case of 2,7-substitutions, making HOMO of P3 insensitive towards geometrical deformations and the corresponding hole mobility being the largest in the series.

As a general conclusion, we have reported here a detailed analysis of the charge-transport properties of six new D-A-D-type compounds containing methoxy-substituted carbazole donors with phenyl or carbazole bridges as acceptors. Our results suggest a delicate balance between the positive and negative effects induced by methoxy substitutions on the hole mobility of organic semiconductors. Given that methyl substituents were found to improve the hole transport as compared to methoxy ones (as in the case of spiro-MeTAD), one could be tempted to avoid using methoxy substituents, or replace them by methyl groups. However, depending on the targeted application of these compounds, and in view of the versatility of positive impacts of methoxy groups on other key parameters for the functioning of devices in organic electronics, this could be a "bad" idea. A nice example recently shown by Sallenave et al., 28 where replacing methoxy groups of spiro-OMeTAD by methyl groups (spiro-MeTAD) resulted in a significant increase in hole mobility by more than five times, while maintain the photovoltaic performances in perovskite solar cells using spiro-MeTAD compounds as hole-transporting material (HTM) only slightly inferior as compared to those based on spiro-OMeTAD, which points to the dominant importance of perovskite-HTM interface properties and to the special role of methoxy groups in this regard.

Consequently, in addition to provide deep insights on the mechanisms by which methoxy groups affect the hole mobility of carbazole-based semiconductors, our results suggest "linear (centrosymmetric) D-A-D architectures" as a helpful design guideline through both introducing methoxy groups in the new semiconductors and by simultaneously avoiding as much as possible the polarity effect on the hole mobility.

Acknowledgements

Dr. Seyhan Salman and Dr. Gjergji Sini acknowledge the Institute of Advanced Studies at University of Cergy-Pontoise for their support of scientific activities. Computational resources were provided by the Supercomputing Center of University of Cergy-Pontoise. This research was funded by the European Social Fund under the No 09.3.3-LMT-K-712 "Development of Competences of Scientists, other Researchers and Students through Practical Research Activities" measure (Project No 09.3.3-LMT-K-712-19-0177).

Conflicts of interest

There are no conflicts of interest to declare.

References

- 1. Uoyama, H.; Goushi, K.; Shizu, K.; Nomura, H.; Adachi, C., Highly efficient organic light-emitting diodes from delayed fluorescence. *Nature* **2012**, *492* (7428), 234-8.
- 2. Wex, B.; Kaafarani, B. R., Perspective on carbazole-based organic compounds as emitters and hosts in TADF applications. *Journal of Materials Chemistry C* **2017**, *5* (34), 8622-8653.
- 3. Lv, X.; Huang, R.; Sun, S.; Zhang, Q.; Xiang, S.; Ye, S.; Leng, P.; Dias, F. B.; Wang, L., Blue TADF Emitters Based on Indenocarbazole Derivatives with High Photoluminescence and Electroluminescence Efficiencies. *ACS Appl Mater Interfaces* **2019**, *11* (11), 10758-10767.
- 4. Jayakumar, J.; Wu, T.-L.; Huang, M.-J.; Huang, P.-Y.; Chou, T.-Y.; Lin, H.-W.; Cheng, C.-H., Pyridine-Carbonitrile-Carbazole-Based Delayed Fluorescence Materials with Highly Congested Structures and Excellent OLED Performance. *ACS Applied Materials & Interfaces* **2019**, *11* (23), 21042-21048.
- 5. Magaldi, D.; Ulfa, M.; Nghiêm, M.-P.; Sini, G.; Goubard, F.; Pauporté, T.; Bui, T.-T. n., Hole transporting materials for perovskite solar cells: molecular versus polymeric carbazole-based derivatives. *Journal of Materials Science* **2020**, *55* (11), 4820-4829.
- 6. Lee, D. Y.; Sivakumar, G.; Manju; Misra, R.; Seok, S. I., Carbazole-Based Spiro[fluorene-9,9'-xanthene] as an Efficient Hole-Transporting Material for Perovskite Solar Cells. *ACS applied materials & interfaces* **2020**, *12* (25), 28246-28252.
- 7. Li, M.; Wang, Z.; Liang, M.; Liu, L.; Wang, X.; Sun, Z.; Xue, S., Low-Cost Carbazole-Based Hole-Transporting Materials for Perovskite Solar Cells: Influence of S,N-Heterocycle. *The Journal of Physical Chemistry C* **2018**, *122* (42), 24014-24024.
- 8. Magomedov, A.; Paek, S.; Gratia, P.; Kasparavicius, E.; Daskeviciene, M.; Kamarauskas, E.; Gruodis, A.; Jankauskas, V.; Kantminiene, K.; Cho, K. T.; Rakstys, K.; Malinauskas, T.; Getautis, V.; Nazeeruddin, M. K., Diphenylamine-Substituted Carbazole-Based Hole Transporting Materials for Perovskite Solar Cells: Influence of Isomeric Derivatives. *Advanced Functional Materials* **2018**, *28* (9), 1704351.
- 9. Wang, H.-Y.; Liu, F.; Xie, L.-H.; Tang, C.; Peng, B.; Huang, W.; Wei, W., Topological Arrangement of Fluorenyl-Substituted Carbazole Triads and Starbursts: Synthesis and Optoelectronic Properties. *The Journal of Physical Chemistry C* **2011**, *115* (14), 6961-6967.
- 10. Huang, H.; Fu, Q.; Pan, B.; Zhuang, S.; Wang, L.; Chen, J.; Ma, D.; Yang, C., Butterfly-Shaped Tetrasubstituted Carbazole Derivatives as a New Class of Hosts for

- Highly Efficient Solution-Processable Green Phosphorescent Organic Light-Emitting Diodes. *Organic Letters* **2012**, *14* (18), 4786-4789.
- 11. Tsai, M.-H.; Ke, T.-H.; Lin, H.-W.; Wu, C.-C.; Chiu, S.-F.; Fang, F.-C.; Liao, Y.-L.; Wong, K.-T.; Chen, Y.-H.; Wu, C.-I., Triphenylsilyl- and Trityl-Substituted Carbazole-Based Host Materials for Blue Electrophosphorescence. *ACS Applied Materials & Interfaces* **2009**, *1* (3), 567-574.
- 12. Matsuoka, K.; Albrecht, K.; Nakayama, A.; Yamamoto, K.; Fujita, K., Highly Efficient Thermally Activated Delayed Fluorescence Organic Light-Emitting Diodes with Fully Solution-Processed Organic Multilayered Architecture: Impact of Terminal Substitution on Carbazole–Benzophenone Dendrimer and Interfacial Engineering. *ACS Applied Materials & Interfaces* **2018**, *10* (39), 33343-33352.
- 13. Grybauskaite-Kaminskiene, G.; Volyniuk, D.; Mimaite, V.; Bezvikonnyi, O.; Bucinskas, A.; Bagdziunas, G.; Grazulevicius, J. V., Aggregation-Enhanced Emission and Thermally Activated Delayed Fluorescence of Derivatives of 9-Phenyl-9H-Carbazole: Effects of Methoxy and tert-Butyl Substituents. *Chemistry A European Journal* **2018**, *24* (38), 9581-9591.
- 14. Huang, J.-F.; Liu, J.-M.; Tan, L.-L.; Chen, Y.-F.; Shen, Y.; Xiao, L.-M.; Kuang, D.-B.; Su, C.-Y., Novel carbazole based sensitizers for efficient dye-sensitized solar cells: Role of the hexyl chain. *Dyes and Pigments* **2015**, *114*, 18-23.
- 15. Schloemer, T. H.; Gehan, T. S.; Christians, J. A.; Mitchell, D. G.; Dixon, A.; Li, Z.; Zhu, K.; Berry, J. J.; Luther, J. M.; Sellinger, A., Thermally Stable Perovskite Solar Cells by Systematic Molecular Design of the Hole-Transport Layer. *ACS Energy Letters* **2019**, *4* (2), 473-482.
- 16. Gao, L.; Schloemer, T. H.; Zhang, F.; Chen, X.; Xiao, C.; Zhu, K.; Sellinger, A., Carbazole-Based Hole-Transport Materials for High-Efficiency and Stable Perovskite Solar Cells. *ACS Applied Energy Materials* **2020**, *3* (5), 4492-4498.
- 17. Li, W.; Otsuka, M.; Kato, T.; Wang, Y.; Mori, T.; Michinobu, T., 3,6-Carbazole vs 2,7-carbazole: A comparative study of hole-transporting polymeric materials for inorganic-organic hybrid perovskite solar cells. *Beilstein J Org Chem* **2016**, *12*, 1401-1409.
- 18. Keruckas, J.; Lygaitis, R.; Simokaitiene, J.; Grazulevicius, J. V.; Jankauskas, V.; Sini, G., Influence of methoxy groups on the properties of 1,1-bis(4-aminophenyl)cyclohexane based arylamines: experimental and theoretical approach. *Journal of Materials Chemistry* **2012**, *22* (7), 3015-3027.
- 19. Mimaite, V.; Grazulevicius, J. V.; Laurinaviciute, R.; Volyniuk, D.; Jankauskas, V.; Sini, G., Can hydrogen bonds improve the hole-mobility in amorphous organic semiconductors? Experimental and theoretical insights. *Journal of Materials Chemistry C* **2015**, *3* (44), 11660-11674.
- 20. Maldonado, J. L.; Bishop, M.; Fuentes-Hernandez, C.; Caron, P.; Domercq, B.; Zhang, Y. D.; Barlow, S.; Thayumanavan, S.; Malagoli, M.; Bredas, J. L.; Marder, S. R.; Kippelen, B., Effect of substitution on the hole mobility of bis(diarylamino)biphenyl derivatives doped in poly(styrene). *Chemistry of Materials* **2003**, *15* (4), 994-999.
- 21. Borsenberger, P. M.; Bassler, H., Concerning the role of dipolar disorder on charge transport in molecularly doped polymers. *Journal of Chemical Physics* **1991**, *95* (7), 5327-5331.

- 22. Borsenberger, P. M.; Gruenbaum, W. T.; Magin, E. H.; Sorriero, L. J., Hole transport in tri-p-tolylamine doped polymers The role of the polymer dipole moment. *Chemical Physics* **1995**, *195* (1-3), 435-442.
- 23. Borsenberger, P. M.; Magin, E. H.; Oregan, M. B.; Sinicropi, J. A., The role of dipole moments on hole transport in triphenylamine-doped polymers. *Journal of Polymer Science Part B-Polymer Physics* **1996**, *34* (2), 317-323.
- 24. Borsenberger, P. M.; Schein, L. B., Hole transport in 1-phenyl-3-((diethylamino)styryl)-5-(p-(diethylamino)phenyl)pyrazoline-doped polymers. *Journal of Physical Chemistry* **1994,** *98* (1), 233-239.
- 25. Gantenbein, M.; Hellstern, M.; Le Pleux, L.; Neuburger, M.; Mayor, M., New 4,4'-Bis(9-carbazolyl)–Biphenyl Derivatives with Locked Carbazole–Biphenyl Junctions: High-Triplet State Energy Materials. *Chemistry of Materials* **2015**, *27* (5), 1772-1779. 26. Sakalyte, A.; Simokaitiene, J.; Tomkeviciene, A.; Keruckas, J.; Buika, G.; Grazulevicius, J. V.; Jankauskas, V.; Hsu, C.-P.; Yang, C.-H., Effect of Methoxy Substituents on the Properties of the Derivatives of Carbazole and Diphenylamine. *The Journal of Physical Chemistry C* **2011**, *115* (11), 4856-4862.
- 27. Srour, H.; Doan, T.-H.; Silva, E. D.; Whitby, R. J.; Witulski, B., Synthesis and molecular properties of methoxy-substituted diindolo[3,2-b:2',3'-h]carbazoles for organic electronics obtained by a consecutive twofold Suzuki and twofold Cadogan reaction. *Journal of Materials Chemistry C* **2016**, *4* (26), 6270-6279.
- 28. Sallenave, X.; Shasti, M.; Anaraki, E. H.; Volyniuk, D.; Grazulevicius, J. V.; Zakeeruddin, S. M.; Mortezaali, A.; Gratzel, M.; Hagfeldt, A.; Sini, G., Interfacial and bulk properties of hole transporting materials in perovskite solar cells: spiro-MeTAD versus spiro-OMeTAD. *Journal of Materials Chemistry A* **2020**, *8* (17), 8527-8539.
- 29. Sallenave, X.; Bucinskas, A.; Salman, S.; Volyniuk, D.; Bezvikonnyi, O.; Mimaite, V.; Grazulevicius, J. V.; Sini, G., Sensitivity of Redox and Optical Properties of Electroactive Carbazole Derivatives to the Molecular Architecture and Methoxy Substitutions. *Journal of Physical Chemistry C* **2018**, *122* (18), 10138-10152.
- 30. Amorim, C. A.; Cavallari, M. R.; Santos, G.; Fonseca, F. J.; Andrade, A. M.; Mergulhão, S., Determination of carrier mobility in MEH-PPV thin-films by stationary and transient current techniques. *Journal of Non-Crystalline Solids* **2012**, *358* (3), 484-491.
- 31. Juška, G.; Genevičius, K.; Viliunas, M.; Arlauskas, K.; Stuchlíková, H.; Fejfar, A.; Kočka, J., New method of drift mobility evaluation in µc-Si:H, basic idea and comparison with time-of-flight. *Journal of Non-Crystalline Solids* **2000**, *266-269*, 331-335.
- 32. Kohn, W.; Sham, L. J., Self-Consistent Equations Including Exchange and Correlation Effects. *Phys. Rev.* **1965**, *140*, A1133-A1138.
- 33. Cossi, M.; Rega, N.; Scalmani, G.; Barone, V., Energies, structures, and electronic properties of molecules in solution with the C-PCM solvation model. *Journal of Computational Chemistry* **2003**, *24* (6), 669-681.
- 34. Klamt, A.; Schüürmann, G., COSMO: a new approach to dielectric screening in solvents with explicit expressions for the screening energy and its gradient. *Journal of the Chemical Society, Perkin Transactions 2* **1993**, (5), 799-805.

- 35. Andzelm, J.; Kölmel, C.; Klamt, A., Incorporation of solvent effects into density functional calculations of molecular energies and geometries. *The Journal of Chemical Physics* **1995**, *103* (21), 9312-9320.
- 36. Cossi, M.; Rega, N.; Scalmani, G.; Barone, V., Polarizable dielectric model of solvation with inclusion of charge penetration effects. *The Journal of Chemical Physics* **2001**, *114* (13), 5691-5701.
- 37. Chai, J. D.; Head-Gordon, M., Long-range corrected hybrid density functionals with damped atom-atom dispersion corrections. *Physical Chemistry Chemical Physics* **2008**, *10* (44), 6615-6620.
- 38. Sun, H.; Ryno, S.; Zhong, C.; Ravva, M. K.; Sun, Z.; Körzdörfer, T.; Brédas, J.-L., Ionization Energies, Electron Affinities, and Polarization Energies of Organic Molecular Crystals: Quantitative Estimations from a Polarizable Continuum Model (PCM)-Tuned Range-Separated Density Functional Approach. *Journal of Chemical Theory and Computation* **2016**, *12* (6), 2906-2916.
- 39. Lee, C. T.; Yang, W. T.; Parr, R. G., Development of the Colle-Salvetti Correlation-Energy Formula into a Functional of the Electron-Density. *Physical Review B* **1988**, *37* (2), 785-789.
- 40. Becke, A. D., Density Functional Thermochemistry. 3. The Role of Exact Exchange. *Journal of Chemical Physics* **1993**, *98* (7), 5648-5652.
- 41. Beljonne, D.; Cornil, J.; Muccioli, L.; Zannoni, C.; Bredas, J.-L.; Castet, F., Electronic Processes at Organic-Organic Interfaces: Insight from Modeling and Implications for Opto-electronic Devices. *Chemistry of Materials* **2011**, *23* (3), 591-609.
- 42. Frisch, M. J.; Trucks, G. W.; Schlegel, H. B.; Scuseria, G. E.; Robb, M. A.; Cheeseman, J. R.; Scalmani, G.; Barone, V.; Mennucci, B.; Petersson, G. A.; Nakatsuji, H.; Caricato, M.; Li, X.; Hratchian, H. P.; Izmaylov, A. F.; Bloino, J.; Zheng, G.; Sonnenberg, J. L.; Hada, M.; Ehara, M.; Toyota, K.; Fukuda, R.; Hasegawa, J.; Ishida, M.; Nakajima, T.; Honda, Y.; Kitao, O.; Nakai, H.; Vreven, T.; Montgomery, J., J. A.; Peralta, J. E.; Ogliaro, F.; Bearpark, M.; Heyd, J. J.; Brothers, E.; Kudin, K. N.; Staroverov, V. N.; Keith, T.; Kobayashi, R.; Normand, J.; Raghavachari, K.; Rendell, A.; Burant, J. C.; Iyengar, S. S.; Tomasi, J.; Cossi, M.; Rega, N.; Millam, J. M.; Klene, M.; Knox, J. E.; Cross, J. B.; Bakken, V.; Adamo, C.; Jaramillo, J.; Gomperts, R.; Stratmann, R. E.; Yazyev, O.; Austin, A. J.; Cammi, R.; Pomelli, C.; Ochterski, J. W.; Martin, R. L.; Morokuma, K.; Zakrzewski, V. G.; Voth, G. A.; Salvador, P.; Dannenberg, J. J.; Dapprich, S.; Daniels, A. D.; Farkas, O.; Foresman, J. B.; Ortiz, J. V.; Cioslowski, J.; Fox, D. J., **2009**, *Gaussian 09*, *Revision B.01*, *Gaussian Inc.*, *Wallingford CT*, *2010*.
- 43. Bassler, H., Charge transport in disordered organic photoconductors A Monte Carlo Simulation Study. *Physica Status Solidi B-Basic Research* **1993**, *175* (1), 15-56.
- 44. Bakhshiev, N. G., Universal Intermolecular Interactions and Their Effect on the Position of the Electronic Spectra of Molecules in Two-Component Solutions. V. Dependence of the Spectra on the Electrical Properties, Dimensions, and Structure of the Molecules Under Stud. *Optics and Spectroscopy* **1962**, *13*, 24.
- 45. Noboru, M.; Yozo, K.; Masao, K., Solvent Effects upon Fluorescence Spectra and the Dipolemoments of Excited Molecules. *Bulletin of the Chemical Society of Japan* **1956**, *29* (4), 465-470.

- 46. Sumalekshmy, S.; Gopidas, K. R., Photoinduced Intramolecular Charge Transfer in Donor–Acceptor Substituted Tetrahydropyrenes. *The Journal of Physical Chemistry B* **2004**, *108* (12), 3705-3712.
- 47. Lippert, E., Dipolmoment und Elektronenstruktur von angeregten Molekülen. *Zeitschrift für Naturforschung A* **1955**, *10* (7), 541-545.
- 48. Bässler, H.; Köhler, A., Charge transport in organic semiconductors. *Topics in current chemistry* **2012**, *312*, 1-65.
- 49. Coropceanu, V.; Cornil, J.; da Silva Filho, D. A.; Olivier, Y.; Silbey, R.; Brédas, J.-L., Charge Transport in Organic Semiconductors. *Chemical Reviews* **2007**, *107* (4), 926-952.